Selective Detection of Intracellular Drug Metabolism by Metal-Organic Framework-Coated Plasmonic Nanowire

Qiang Zhang, Taku Murasugi, Kotomi Watanabe, Han Wen, Ya Tian, Monica Ricci, Susana Rocha, Tomoko Inose, Hitoshi Kasai, Farsai Taemaitree, Hiroshi Uji-i, Kenji Hirai, and Beatrice Fortuni**

Q. Zhang, T. Murasugi, K. Watanabe, H. Wen, Y. Tian, K. Hirai and H. Uji-i
Research Institute for Electronic Science (RIES), Hokkaido University, N20W10, Sapporo, Hokkaido 001–0020, Japan.
E-mail: hirai@es.hokudai.ac.jp
M. Ricci, S. Rocha, H. Uji-i and B. Fortuni
Department of Chemistry, KU Leuven, Celestijnenlaan 200F, B–3001 Leuven, Belgium.
E-mail: beatrice.fortuni@kuleuven.be
T. Inose, and H. Uji-i
Institute for Integrated Cell-Material Science (WPI-iCeMS), Kyoto University, Yoshida, Sakyo-ku, Kyoto 606-8501, Japan.
H. Kasai, and F. Taemaitree
Institute of Multidisciplinary Research for Advanced Materials (IMRAM), Tohoku University, 2–1–1 Katahira, Aoba–Ward, Sendai 980–8577, Japan.

Keywords: metal-organic frameworks, nanowire endoscopy, surface-enhanced Raman scattering, intracellular drug metabolism

Unveiling intracellular drug metabolism is crucial for improving drug development, which requires real-time detection with molecular selectivity in the intracellular environment. Surface-enhanced Raman scattering (SERS) with metal nanoparticles enables the detection of molecules in living cells, but after entering the cells, most nanoparticles are captured into vesicles, limiting the SERS detection inside these compartments. Moreover, the identification of the target signal in the complex intracellular environment is challenging due to Raman fingerprints from endogenous material, interfering with the drug signal. To overcome these issues, here we report the coating of a silver nanowire with zeolitic imidazolate framework-8 (ZIF-8) as a novel endoscopic probe with molecular selectivity to investigate the location and metabolism in cells of a common anticancer drug, irinotecan. Irinotecan in cells is metabolized by carboxylesterase

to form SN-38, which inhibits topoisomerase I and DNA synthesis. Thanks to the molecular selectivity of ZIF-8, the endoscopic probe selectively adsorbs and detects SERS signal of SN-38 over irinotecan. This selectivity enabled to monitor the conversion of irinotecan into SN-38 and follow its intracellular location over time. This work clearly shows the potential of MOF-coated nanowire endoscopy to specifically track drug molecules and explore their metabolism in cells.

1. Introduction

Studying the metabolism of drug molecules in cells assists in determining their mechanism of action and consequently improves the rational design of new therapeutic agents.[1] To this end, real-time and non-invasive detection methods with high selectivity towards active drug molecules in complex cellular environments are required. As a sensing method, fluorescence-based techniques have been applied to monitor drugs inside cells.[2] Nevertheless, their performance is often affected by cell autofluorescence, or photoquenching or photobleaching of the target molecule upon chemical interactions with biomolecules. Surface-enhanced Raman scattering (SERS) has been proposed as an alternative approach to fluorescence.[3] SERS measurements inside living cells are typically performed using metal nanoparticles (NPs). The NPs, however, remain in vesicles after cellular uptake,[4] limiting the detection of the SERS signal to the vesicle compartments. These conventional methods are accordingly disqualified for real-time and non-invasive detection of the metabolism of drug molecules in cellular environments.

Alternatively, plasmonic nanowire endoscopy has been recently developed to collect SERS signals of molecules in living cells.[5] In this approach, an endoscopy probe based on silver nanowires is mechanically inserted into a single living cell, and SERS signals are collected from specific cell compartments by adjusting the location of the nanowire. Despite being promising, the endoscopic probe exhibits the inherent disadvantage of SERS that it is not selective towards the target drug molecule in living cells. Consequently, during the measurements, the spectra of all molecules surrounding the probe are acquired, producing big data sets from which spectral identification is challenging. Furthermore, chemical interactions of the target molecule with endogenous materials increase the complexity of the spectra obtained. These shortcomings indicate that an innovation enabling specific drug detection is imperative to apply SERS for studying drug metabolism in living cells.

To overcome these issues, we endow the SERS-based nanowire endoscopy technique with molecular specificity by coating the nanowire endoscopic probe with a metal-organic

framework (MOF). MOFs are porous crystalline materials constructed from metal ions linked by organic ligands, which have a wide range of applications.[6] Thanks to their highly regulated porous structures, MOFs can filter and selectively accommodate specific molecules.[7] Coating

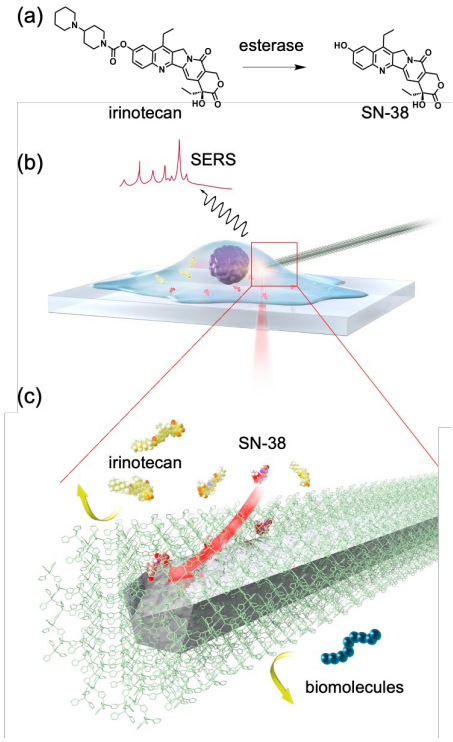

Scheme 1. (a) Reaction scheme of hydrolysis of irinotecan into SN-38, its active moiety, by esterase. (b) Schematic illustration of MOF-coated nanowire endoscopy. In cells, irinotecan, the anticancer prodrug, is hydrolyzed into SN-38, the active drug. SN-38 can be detected in the intracellular environment via SERS using MOF-coated silver nanowire as endoscopic probes. (c) Schematic illustration of selective detection of MOF-coated nanowire probe inside cells. SN-38 (red) is selectively adsorbed by the MOF coating, instead of irinotecan (yellow) and biomolecules (blue), and diffuse to the surface of the silver nanowire, where SERS signals of SN-38 are detected, providing information on intracellular hydrolysis of irinotecan and localization of SN-38.

the metallic surface of a silver nanowire with a MOF would provide the probe with the capability of capturing specific drug molecules in living cells (preventing random molecules from diffusing through the porous network[8]). In this way, the probe still maintains the plasmonic effect on the metal surface when detecting SERS spectra of the adsorbed drug molecules.

In this work, we demonstrated the application of MOF-coated endoscopic probe for the selective detection of drugs and the monitoring of the intracellular conversion of prodrug into

active drug, aiming to address the long-standing issue of distinguishing a drug from its prodrug in the cellular environment. As a model for this study, we chose irinotecan-to-SN-38 conversion. Irinotecan is an anticancer therapeutic agent, widely used in the clinic for the treatment of colorectal, ovarian, pancreatic, gastric tumors.[9] Once inside cancer cells, irinotecan is hydrolyzed by carboxylesterase into the therapeutically active drug of SN-38, which is smaller and more hydrophobic than irinotecan.[10] The main action mechanism of SN-38 is associated with the inhibition of topoisomerase I and consequent irreversible DNA damage.[10] Here, we demonstrated the selective intracellular detection of SN-38 in cells, after enzymatic conversion, using MOF-coated nanowire endoscopy (Scheme 1). By combining the high spatiotemporal resolution and the non-invasiveness of the endoscopic approach with the molecular selectivity of the MOF coating, the proposed technique enabled the localization of SN-38 in HeLa cells and dynamics of enzyme-mediated cleavage of irinotecan. The results proved the applicability of MOF-coated nanowire endoscopy for the real-time monitoring of drug metabolism in living cells. This cutting-edge methodology unlocks new avenues for the field of intracellular drug tracing, offering an indispensable tool in biological spectroscopy and pharmaceutical science.

2. Results and Discussion

Monitoring the conversion of inactive prodrugs into active drugs and revealing the resulting spatial location of drug molecules in cells would contribute to elucidating their mechanism of action and improving their therapeutic efficiency. In this study, irinotecan has been chosen as a prodrug model as it is known to be hydrolyzed into its therapeutic moiety, SN-38, by carboxylesterase in the intracellular environment (Scheme 1). The structural analogy of irinotecan and SN-38 gives rise to very similar SERS fingerprints (Figure S1), which are even harder to be distinguished in the heterogeneous cellular environment. SN-38 is smaller and more hydrophobic than irinotecan (Figure S2 and Table S1)[10]. Their difference in hydrophobicity and size can, therefore, be used as a discriminating factor to differentiate the two species. For this purpose, silver nanowires were coated with ZIF-8, and their size/polarity selectivity was first evaluated in solution. Then, the MOF-coated nanowires were used for the endoscopy experiments in cells.

2.1. Fabrication and Characterization of AuAgNW@ZIF-8.

Silver nanowires (AgNWs) were synthesized using a previously reported method.[5c] In reported studies, it has been demonstrated that the SERS sensitivity of the AgNWs is enhanced after roughing the smooth nanowire surface through galvanic replacement reaction (GRR).[5b, 11] In this work, GRR was therefore used to increase the density of plasmonic coupling points on the

silver nanowire for an enhanced SERS sensitivity. The obtained nanowires were denoted as AuAgNWs. Scanning electron microscopy (SEM) and scanning transmission electron microscopy (STEM) images show the smooth surface of AgNWs before GRR (Figure S3a-c), and the rough surface with concave areas of the nanowire after GRR (AuAgNWs, Figure S3d-f). The reproducibility of the AuAgNWs obtained by GRR is shown in Figure S4. A small amount of Au was detected on AuAgNWs by energy-dispersive X-ray spectroscopy (EDS) and inductively coupled plasma optical emission spectroscopy (ICP-OES) (Figure S5). The maximum of the extinction band was red-shifted from 389 nm to 449 nm after GRR (Figure S6a). Apart from this shift, however, no remarkable difference could be observed on the plasmonic band around the visible region (532 nm or 633 nm).

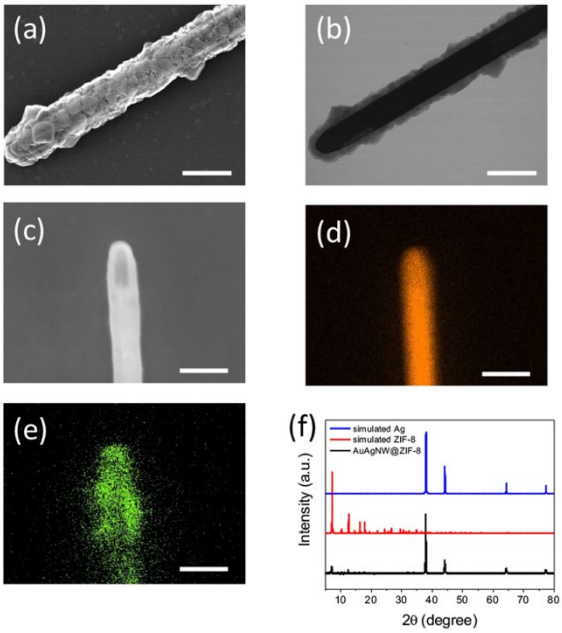

Figure 1. Characterization of AuAgNW@ZIF-8. STEM images of AuAgNW@ZIF-8: (a) SE and (b) TE models. (c) SEM image of AuAgNW@ZIF-8. EDS mappings of AuAgNW@ZIF-8: (d) Ag and (e) Zn. XRD patterns of (f) AuAgNW@ZIF-8 and simulated Ag and ZIF-8. Scale bar: 500 nm.

To compare their SERS performance, the AgNWs and the AuAgNWs were modified with a Raman reporter, 4-mercaptobenzoic acid (4-MBA), and SERS mappings of the molecules were collected (Figure S6b). The SERS maps showed that AuAgNWs had better SERS performance (high SERS signal and high density of coupling points) compared to the original AgNW for both wavelengths (633 nm and 532 nm). Since living cells were investigated in this study, to

minimize autofluorescence phenomena and reduce the photodamage to the cells, 633 nm wavelength laser was chosen for the Raman measurements.

When compared to the smooth AgNW, the SERS signal from 4-MBA on the single AuAgNW displayed an enhancement factor of 10^5 upon 633 laser excitation (the details for the calculation are described in SI).

To implement the endoscopic probe with selective adsorption capability, AuAgNWs were coated with zeolitic imidazolate framework-8 (ZIF-8). ZIF-8 is one of MOFs used for molecular sieving and bio-applications because of the molecular separation capability and chemical stability.[7a, 8c, 12] The ZIF-8 coating procedure was performed by mixing AuAgNWs with the ZIF-8 precursor solution in an ice bath. Coating of the AuAgNWs with ZIF-8 was confirmed using SEM and STEM. As depicted in Figure 1a-b, ZIF-8 crystals were observed on the surface of MOF-coated AuAgNWs (AuAgNW@ZIF-8). The shell was characterized by EDS and X-ray diffraction analysis (XRD) (Figure 1c-f). The Zn element is observed in the element mapping and the energy spectrum (Figure 1e and Figure S7). Figure 1f shows the obtained XRD patterns of AuAgNW@ZIF-8, together with the simulated patterns for Ag and ZIF-8 crystals. The peaks at approximately 7.3° and 12.7° (2θ) correspond to the (110) and (211) planes overlapped with the standard XRD patterns of ZIF-8 crystals, which is identified as the ZIF-8 shell on the AuAgNWs.[13] The peaks at around 38.1°, 44.3°, 64.4°, and 77.4° (2θ), that corresponded to the (111), (200), (220), and (311) planes, respectively, are consistent with the XRD patterns of Ag, which is identified as the AgNW core.[14] These results confirmed the

growth of ZIF-8 on AuAgNW by coordination bonding to form the core-shell structure of AuAgNW@ZIF-8.

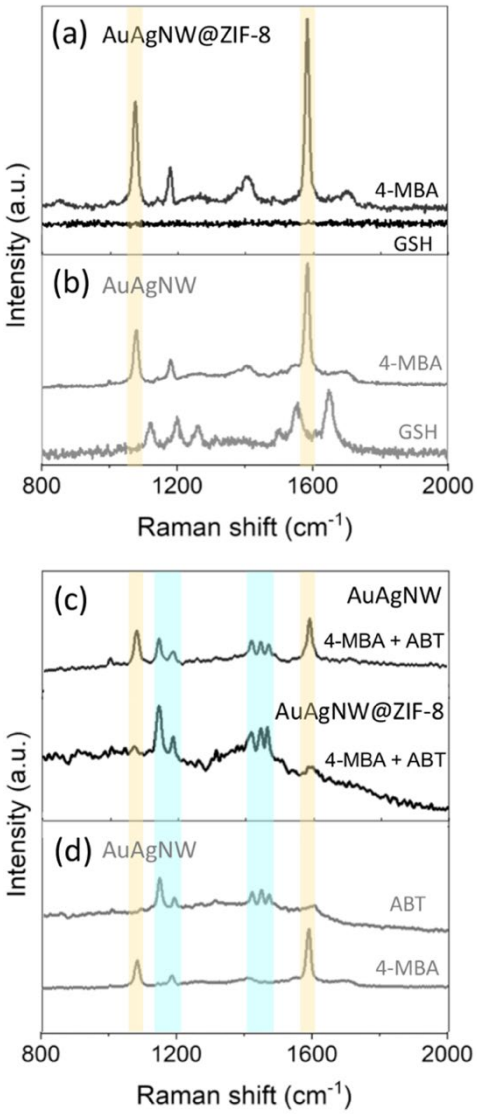

Figure 2. Molecular Selectivity of AuAgNW@ZIF-8. SERS spectra of 4-MBA and GSH on (a) AuAgNW@ZIF-8 and on (b) AuAgNW, respectively. (c) SERS spectra of the mixture of 4-MBA and GSH on AuAgNW (top) and on AuAgNW@ZIF-8 (bottom). (d) Reference SERS spectra of 4-MBA and ABT taken individually on AuAgNW.

2.2. Molecular Selectivity of AuAgNW@ZIF-8.

The exclusion of endogenous peptides from SERS detection is of importance when performing intracellular endoscopy. Glutathione (GSH) is a common intracellular thiol-containing peptide associated with many biological processes,[15] it was therefore chosen as endogenous peptide to evaluate the molecular selectivity of AuAgNW@ZIF-8. To this purpose, the adsorption of GSH

on AuAgNW@ZIF-8 was compared with that of 4-MBA. As shown in Figure S2 and Table S1, the molecular size of 4-MBA is estimated to be 6.8 × 3.6 Å.

On the other hand, the molecular size of GSH cannot be defined because of the flexible structure, but the most stable configuration of GSH is estimated to be 9.2 × 6.4 Å, which is relatively larger than 4-MBA. Additionally, the partition coefficient (log *P*) of 4-MBA and GSH are calculated to be 1.78 and -3.23, respectively, indicating that 4-MBA is more hydrophobic than GSH. AuAgNW@ZIF-8 or AuAgNWs were immersed in a solution containing 4-MBA or GSH, respectively. In the case of AuAgNW@ZIF-8, only the SERS spectrum of 4-MBA was recorded (Figure 2a). Differently, both 4-MBA and GSH signals were detected on non-coated AuAgNWs (Figure 2b). This indicates that small hydrophobic molecules, such as 4-MBA, could diffuse across the ZIF-8 coating and access the nanowire surface, whereas larger and more hydrophilic molecules, such as GSH, could not penetrate the ZIF-8 layer. In agreement with these results, a previous study also showed that ZIF-8 presents a molecular sieving effect, typically, accommodating molecules in the 0.4 — 0.6 nm size range[16]. It should be noted that the ZIF-8 shell was not damaged/altered by the 4-MBA adsorption process (Figure S8), suggesting that the detection selectivity is directly attributed to the presence of the ZIF-8 shell. In the case of GSH, one of the factors which likely hinders its adsorption on AuAgNW@ZIF-8 is the relatively bulky structure of GSH with the size of 9.2 × 6.4 Å (Table S1 and Figure S2). Moreover, the lower hydrophilicity of GSH can also plays a key role on the selectivity. As given in Table S1, the partition coefficient of GSH is -3.23, which indicates that GSH molecules are more hydrophilic compared to 4-MBA. The pores of ZIF-8 are instead highly hydrophobic,[17] resulting in a very low affinity with the tripeptide, GSH.

To further evaluate the selective detection capability of AuAgNW@ZIF-8, an even higher hydrophobicity was investigated. To this end, 6-(4-(phenyldiazenyl) phenoxy) hexane-1-thiol (ABT) was tested. The molecular size of ABT is estimated to be 8.3 × 4.3 Å, although the precise size of ABT cannot be defined because of the flexible alkyl chains. The partition coefficient of ABT is calculated to be 10.5 (Table S1 and Figure S2), which indicates a much higher hydrophobicity than 4-MBA. In the case of AuAgNWs (without the ZIF-8 coating), the SERS fingerprints of both 4-MBA and ABT were observed simultaneously on the same spectrum (Figure 2c, top). Whereas, on the AuAgNW@ZIF-8, the dominant SERS peaks from the mixture are attributed to ABT, while only very weak SERS peaks corresponding to 4-MBA are detected (Figure 2c, bottom). This clearly indicates that ABT molecules were preferentially adsorbed over 4-MBA into the ZIF-8 shell and therefore favorably detected during the SERS measurements. As being ZIF-8 a hydrophobic porous material,[17] hydrophobic ABT has a

strong affinity to be adsorbed into the pores. For a reference, SERS spectra of 4-MBA and ABT were individually taken from AuAgNWs (Figure 2d). These results suggest that AuAgNW@ZIF-8 preferentially adsorbs hydrophobic molecules.

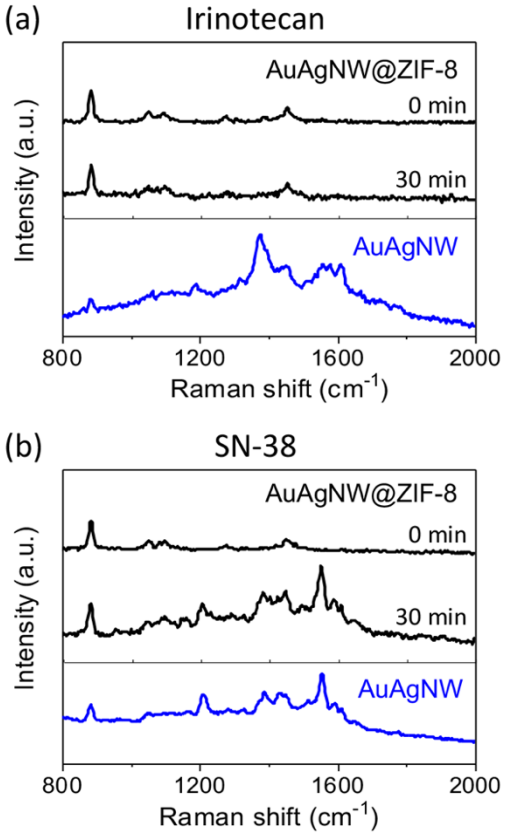

Figure 3. Adsorption and SERS detection of irinotecan and SN-38 on AuAgNW@ZIF-8. (a) SERS spectra of irinotecan in ethanol using AuAgNW@ZIF-8 at 0 min and 30 min (black), and using AuAgNW (blue). (b) SERS spectra of SN-38 in ethanol using AuAgNW@ZIF-8 at 0 min and 30 min (black), and using AuAgNW (blue).

2.3. Adsorption and Detection of Irinotecan and SN-38 on AuAgNW@ZIF-8.

To test the feasibility of the proposed method for the intracellular formation and localization of SN-38, the capability of AuAgNW@ZIF-8 to discriminate between irinotecan and SN-38 was first verified *in vitro*. In this test, ethanol solutions of irinotecan or SN-38 (1 mM) were used because SN-38 solubility in water is very limited. In the case of non-coated AuAgNW, (Figure 3a and 3b, blue lines), both irinotecan and SN-38, could be individually detected. In contrast, when using AuAgNW@ZIF-8, only Raman signals from the solvent (ethanol) (882, 1064, 1092, 1277, 1455 cm^{-1}) are detected after immersion of the probe in both solutions, respectively (Figure 3a-b, black lines). In the case of irinotecan solution, even after 30 min from the

immersion, only ethanol fingerprint is observed, with no SERS signal from irinotecan being detected (Figure 3a). However, when the probe was immersed in a solution of SN-38, after 30 min, clear Raman peaks from SN-38 appeared (Figure 3b). These peaks (1190, 1390 and 1560 cm^{-1}) are assigned to the ring breathing and stretching of SN-38.[18] The results obtained from these measurements show that when AuAgNW are coated with ZIF-8, SN-38 molecules can pass through the pores of the ZIF-8 and reach the AuAgNW surface to be detected by SERS, while irinotecan molecules cannot be adsorbed (excluding irinotecan from the detection). As shown in Figure S2 and Table S1, the size of irinotecan (15.7 × 8.7 Å) is slightly larger than SN-38 (11.7 × 7.3 Å). Additionally, SN-38 has higher hydrophobicity, with log *P* of ~1.84, which enables SN-38 to be adsorbed by ZIF-8 over irinotecan.

Before monitoring the irinotecan-SN-38 enzymatic conversion and localization in cells, the selective detection of SN-38 over irinotecan after hydrolysis was tested *in vitro*. AuAgNW@ZIF 8 was mixed with an irinotecan solution containing esterase derived from a pig liver (PLE). PLE is known to hydrolyze carboxylic acid esters.[19] In this experiment, it was used to mimic the enzymatic digestion of irinotecan, which in cells occurs via intracellular esterase. SERS signals were collected from AuAgNW@ZIF-8/irinotecan/PLE solution at different time points (0, 5, 20, and 30 min) (Figure S9). Thanks to the selectivity of ZIF-8 coating, only SERS signals from SN-38 could be observed, and, most importantly, no signal was observed before PLE addition. The integrity of the ZIF-8 shell was verified upon incubation with PLE-containing aqueous solution, no damage was observed (Figure S10). The successful detection of irinotecan conversion into SN-38 using AuAgNW@ZIF-8 *in vitro* demonstrates that they can perform intracellular investigation of SN-38. AuAgNW@ZIF-8 was then used for the fabrication of endoscopic probes.

2.4. Fabrication of AuAgNW@ZIF-8 Endoscopic Probes.

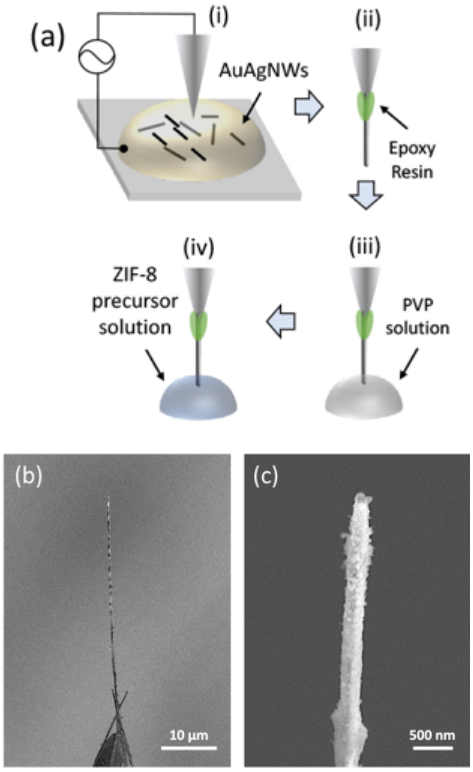

Figure 4. (a) Schematic illustration of the fabrication of AuAgNW@ZIF-8 endoscopic probe: AuAgNWs attachment to W tip via AC dielectrophoresis (i), gluing of the tip with epoxy resin (ii), PVP modification (iii), coating with ZIF-8 shell (iv). (b, c) SEM images of AuAgNW@ZIF 8 probe at different magnifications.

The endoscopy probes are typically prepared by attaching nanowires to a tungsten (W) tip by alternating current (AC) dielectrophoresis. Because AuAgNW@ZIF-8 cannot be attached to W tip by the AC dielectrophoresis due to the presence of ZIF-8 shell, ZIF-8 shell was grown on AuAgNW after their attachment to the W tip (Figure 4a). Thus, the coating protocol was slightly modified. Similar to our reported protocols,[5] AuAgNWs were attached to a sharpened W tip using AC dielectrophoresis. Afterward, the AuAgNWs were fixed on the W tip by gluing the junction with epoxy resin to prevent its detaching during the probe insertion into cells. In this work, the AuAgNWs on the W tip was coated with polyvinylpyrrolidone (PVP) which possesses coordination sites to induce the growth of ZIF-8. Finally, the AuAgNWs endoscopic probe was immersed in a ZIF-8 precursor solution to form the ZIF-8 shell. The SEM images in Figure 4b and 4c show the presence of the ZIF-8 shell on the AuAgNW endoscopic probe (EDS analysis is shown in Figure S11).

After confirming the presence of ZIF-8 on AuAgNW, the homogeneity of the shell formation was confirmed to prevent false detection of irinotecan. To this end, the endoscopic probe was first inserted into an irinotecan solution (PLE-free), and SERS spectra were collected. The SERS signals obtained do not present any fingerprint related to irinotecan (Figure 5a, black line), meaning that ZIF-8 shell successfully shields AuAgNW surface from irinotecan molecules. On the contrary, after PLE was added into the irinotecan solution, the SERS signals of SN-38 were distinctly observed after 1 h incubation (Figure 5a, red line), confirming the selective sensing ability of the AuAgNW@ZIF-8-based endoscopic probes towards SN-38 molecules upon enzymatic hydrolysis of irinotecan. Considering that the dosage of anticancer drugs in the clinical application is maintained very low, the sensitivity threshold of our probe was verified. Figure 5b shows that the SN-38 fingerprint was clearly observed at 10^{-5} M and could still be distinguished at 10^{-7} M, evidently proving a high sensitivity.

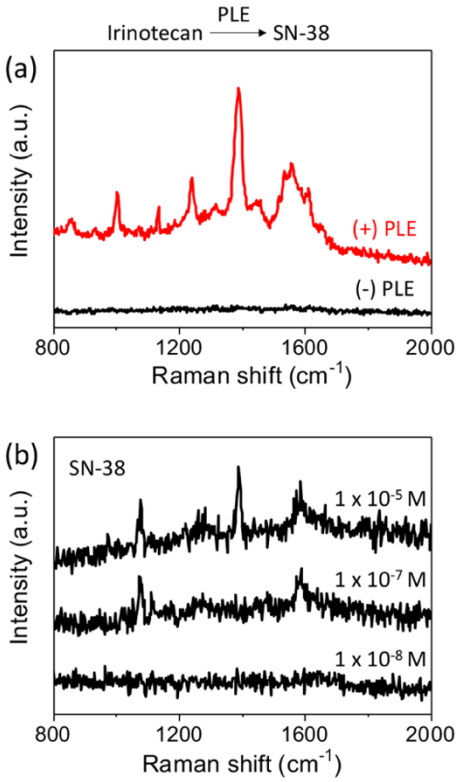

Figure 5. (a) Enzymatic conversion of irinotecan into SN-38 in aqueous solution: SERS spectra of irinotecan incubated with PLE for 1 h (red) and without PLE (black) using AuAgNW@ZIF-8. (b) SERS spectra of different concentrations of SN-38 in aqueous solution using AuAgNW@ZIF-8: 10^{-5} M, 10^{-7} M and 10^{-8} M. SN-38 ethanol solution was added to water surrounding AuAgNW@ZIF-8 to obtain the target concentrations.

2.5. Detection of Irinotecan-to-SN-38 Conversion via AuAgNW@ZIF-8 Endoscopy in Living Cells.

To monitor the prodrug-to-drug conversion *in cellulo*, AuAgNW@ZIF-8 endoscopic probe was site-specifically inserted into a HeLa cell after irinotecan administration. The presence of SN-38 molecules coming from the intracellular enzymatic hydrolysis of irinotecan was then detected over time. The probe was individually inserted into the cytoplasm or the nucleus (Figure 6a-b, respectively) of a HeLa cell treated with irinotecan at different incubation times: 1, 3, 5 and 24 h. After the probe insertion, the laser was focused on the AuAgNW@ZIF-8 probe, and SERS spectra were collected from the cytoplasm or the nucleus. Note that the probe only stays in the cell for the recording of the spectra, which only takes a few minutes, afterwards it is retracted. For each time point, 10 cells were investigated. The representative spectra are displayed in Figure 6c-d. SEM images of the AuAgNW@ZIF-8 probe were collected after the endoscopy measurements to verify that ZIF-8 shell was not decomposed in the cellular environment (Figure S12). The SERS spectra collected from the endoscopy did not show any signals within 1 h of incubation with irinotecan neither in the cytoplasm nor the nucleus (Figure 6c-d, grey lines). This indicates that SN-38 production upon irinotecan hydrolysis was still below the detection limit of our method (10^{-7} M). Differently, at 3 h, weak SN-38 peaks appeared in the spectra recorded from the cytoplasm, while still no signals were detected in the nucleus (Figure 6c-d, black lines). This can be explained by the fact that esterase-mediated hydrolysis mainly occurs in the cytoplasm (rather than in the nucleus).[20] At 5 h, the SN-38 fingerprint becomes more intense in the cytoplasm and could be finally observed in the nucleus (Figure 6c-d, red lines). These data suggest that, after 5 h of incubation, a considerable number of SN-38 molecules ($> 10^{-7}$ M) coming from the cytoplasm has reached the nucleus, where SN-38 performs its therapeutic action. Interestingly, at 24 h incubation time, SERS signals of SN-38 were no longer detectable in the cytoplasmic region by our endoscopic probes (Figure 6c, blue line). This is most likely attributed to two competing processes, (i) the diffusion of SN-38 molecules into the nucleus and (ii) the excretion of both SN-38 and irinotecan molecules from the cells by drug efflux pumps (*e.g.*, ABC transporters)[21]. Nevertheless, some weak SN-38 signal was still recorded from the nucleus (Figure 6d, blue line): the decrease of SN-38 SERS intensity in the nucleus at 24 h incubation time can be associated with SN-38 interaction with topoisomerase I.[10]

Endoscopy experiments were performed in untreated HeLa cells as a control to confirm that no similar SERS spectra could be recorded in the absence of irinotecan. In agreement with previous studies on ZIF-8-coated NPs related to cells,[22] no SERS signals from endogenous cellular

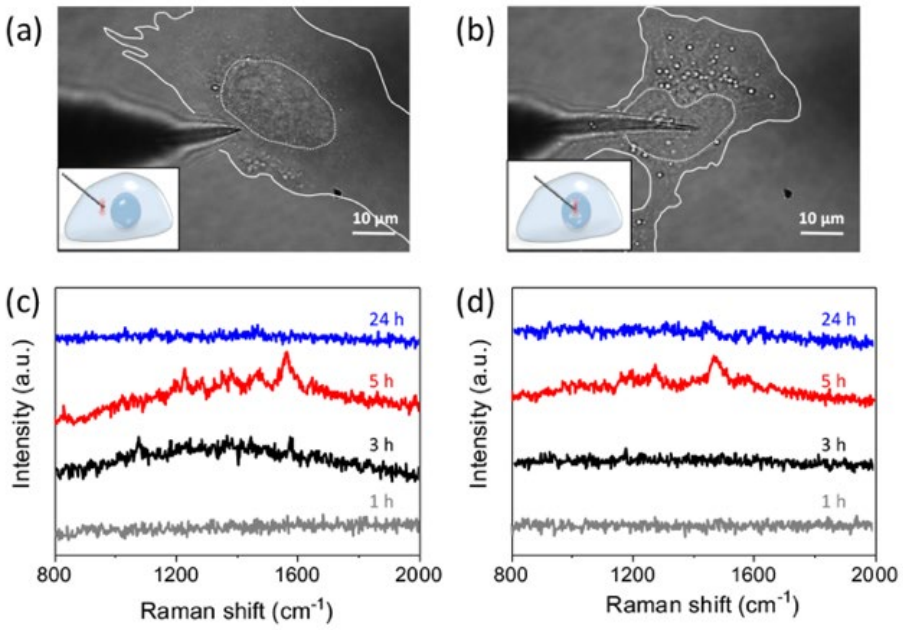

Figure 6. Detection of Irinotecan-to-SN-38 Conversion via AuAgNW@ZIF-8 Endoscopy in Living Cells. Optical microscope images of the probe inserted into (a) the cytoplasm and (b) the nucleus of a living HeLa cell (insets showing the schematic illustrations of the probe insertion). SERS spectra collected in irinotecan-treated HeLa cells at different time points from (c) the cytoplasm and (d) the nucleus. The probe only stays in the cell for several minutes, the time to collect SERS spectra, afterwards it is retracted.

items were collected from the probe, neither in the cytoplasm nor in the nucleus (Figure S13). On the other hand, endoscopy experiments were also performed using AuAgNWs (without ZIF-8 coating) in the nucleus of HeLa cells with and without irinotecan treatment (Figure S14). The spectra obtained showed an extremely high variability presenting series of unassignable SERS peaks. These results evidently indicate that without a ZIF-8 coating on AuAgNWs, the investigation of irinotecan metabolism in living cells via endoscopy could not be performed.

3. Conclusion

In summary, we successfully demonstrated that the AuAgNW@ZIF-8 endoscopic probe selectively detected target molecules inside living cells, being a promising method to monitor drug metabolism and localization in cells. By synergizing the spatiotemporal resolution of silver nanowire endoscopy and the molecular selectivity of the MOF coating, the enzymatic conversion of irinotecan into SN-38 and SN-38 intracellular localization was carefully investigated in HeLa cells over time. For the first time, here, we proved that this kind of

intracellular study could be performed by SERS endoscopy without interference from endogenous biomolecules. This method could be applied to the real-time monitoring of a wide range of drug molecule metabolism, leading to further development and improvement of drug molecule design.

Author Contributions

QZ papered and analyzed AuAgNW@ZIF-8 probes, conducted the cell endoscopy measurements and wrote the paper. TM papered and analyzed AuAgNW@ZIF-8. KW papered and analyzed AuAgNW@ZIF-8 probes, conducted the cell endoscopy measurements. HW supported characterization. YT helped with endoscopy measurements. BF optimized the endoscopic probe preparation and contributed to the writing of the manuscript. TI supported the preparation and characterization of the AuAgNWs. SR optimized the endoscopic probe preparation and contributed to the writing of the manuscript. HK initiated the project and contributed to the writing of the manuscript. FT calculated the size and the and partition coefficients and contributed to the writing of the manuscript. KH, BF and HU initiated and supervised the project, and contributed to the writing of the manuscript. All the authors proofread and approved the final manuscript for submission.

Acknowledgements

This work was supported by JSPS Kakenhi (Grants JP 19KK0136, JP 20K21200, JP 20K05413, JP 21H04634, JP 22H00328) and Research foundation of Flanders (FWO) research grant (G081916N). T.I. thanks to JST PRESTO (JPMJPR2104). B.F. acknowledge Research foundation of Flanders (FWO) for her postdoctoral fellowships (12X1419N and 12X1423N). We thank the Open Facility, Global Facility Center, Creative Research Institution, Hokkaido University for allowing us to use SEM, STEM and XRD. This collaborative work was greatly supported by JSPS Core-to-Core Program A, Advanced Research Networks.

Received: ((will be filled in by the editorial staff))
Revised: ((will be filled in by the editorial staff))
Published online: ((will be filled in by the editorial staff))

References

[1] A. F. Stepan, V. Mascitti, K. Beaumont, A. S. Kalgutkar, *MedChemComm* **2013**, 4, 631.

[2] N. S. White, R. J. Errington, *Adv. Drug Deliv. Rev.* **2005**, 57, 17.

[3] a)K. Koike, K. Bando, J. Ando, H. Yamakoshi, N. Terayama, K. Dodo, N. I. Smith, M. Sodeoka, K. Fujita, *ACS Nano* **2020**, 14, 15032; b)Y. Shen, J. Yue, W. Xu, S. Xu, *Theranostics* **2021**, 11, 4872; c)C. Zong, M. Xu, L. J. Xu, T. Wei, X. Ma, X. S. Zheng, R. Hu, B. Ren, *Chem Rev* **2018**, 118, 4946.

[4] K. Remaut, V. Oorschot, K. Braeckmans, J. Klumperman, S. C. De Smedt, *J. Control. Release* **2014**, 195, 29.

[5] a)Q. Zhang, T. Inose, M. Ricci, J. Li, Y. Tian, H. Wen, S. Toyouchi, E. Fron, A. T. Ngoc Dao, H. Kasai, S. Rocha, K. Hirai, B. Fortuni, H. Uji-i, *ACS Appl. Nano Mater.* **2021**, 4, 9886; b)M. Ricci, B. Fortuni, R. Vitale, Q. Zhang, Y. Fujita, S. Toyouchi, G. Lu, S. Rocha, T. Inose, H. Uji-i, *Anal. Chem.* **2021**, 93, 5037; c)G. Lu, H. De Keersmaecker, L. Su, B. Kenens, S. Rocha, E. Fron, C. Chen, P. Van Dorpe, H. Mizuno, J. Hofkens, J. A. Hutchison, H. Uji-i, *Adv. Mater.* **2014**, 26, 5124.

[6] a)H. Furukawa, K. E. Cordova, M. O'Keeffe, O. M. Yaghi, *Science* **2013**, 341, 1230444; b)S. Kitagawa, R. Kitaura, S.-i. Noro, *Angew. Chem. Int. Ed.* **2004**, 43, 2334; c)G. Férey, *Chem. Soc. Rev.* **2008**, 37, 191; d)J. Liu, W. Zhou, J. Liu, I. Howard, G. Kilibarda, S. Schlabach, D. Coupry, M. Addicoat, S. Yoneda, Y. Tsutsui, T. Sakurai, S. Seki, Z. Wang, P. Lindemann, E. Redel, T. Heine, C. Wöll, *Angew. Chem. Int. Ed.* **2015**, 54, 7441; e)Z. Zhou, S. Mukherjee, S. Hou, W. Li, M. Elsner, R. A. Fischer, *Angew. Chem. Int. Ed.* **2021**, 60, 20551; f)O. Shekhah, H. Wang, D. Zacher, R. A. Fischer, C. Wöll, *Angew. Chem. Int. Ed.* **2009**, 48, 5038; g)R. Ricco, P. Wied, B. Nidetzky, H. Amenitsch, P. Falcaro, *Chem. Commun.* **2020**, 56, 5775.

[7] a)S. Ji, Y. Chen, S. Zhao, W. Chen, L. Shi, Y. Wang, J. Dong, Z. Li, F. Li, C. Chen, Q. Peng, J. Li, D. Wang, Y. Li, *Angew. Chem. Int. Ed.* **2019**, 58, 4271; b)H. Lai, G. Li, F. Xu, Z. Zhang, *J. Mater. Chem. C* **2020**, 8, 2952; c)Z. R. Herm, E. D. Bloch, J. R. Long, *Chem. Mater.* **2014**, 26, 323.

[8] a)T. Li, J. E. Sullivan, N. L. Rosi, *J. Am. Chem. Soc.* **2013**, 135, 9984; b)K. Hirai, S. Furukawa, M. Kondo, H. Uehara, O. Sakata, S. Kitagawa, *Angew. Chem. Int. Ed.* **2011**, 123, 8207; c)X. Liu, L. He, J. Zheng, J. Guo, F. Bi, X. Ma, K. Zhao, Y. Liu, R. Song, Z. Tang, *Adv. Mater.* **2015**, 27, 3273.

[9] B. Yue, R. Gao, Z. Wang, W. Dou, *Front. Cell. Infect. Microbiol.* **2021**, 11:710945.

[10] D. R. Principe, P. W. Underwood, M. Korc, J. G. Trevino, H. G. Munshi, A. Rana, *Front. Oncol.* **2021**, 11:688377.

[11] N. L. Netzer, C. Qiu, Y. Zhang, C. Lin, L. Zhang, H. Fong, C. Jiang, *Chem Commun* **2011**, 47, 9606.

[12] a)G. Lu, S. Li, Z. Guo, O. K. Farha, B. G. Hauser, X. Qi, Y. Wang, X. Wang, S. Han, X. Liu, J. S. DuChene, H. Zhang, Q. Zhang, X. Chen, J. Ma, S. C. J. Loo, W. D. Wei, Y. Yang, J. T. Hupp, F. Huo, *Nat. Chem.* **2012**, 4, 310; b)S. Yuan, L. Feng, K. Wang, J. Pang, M. Bosch, C. Lollar, Y. Sun, J. Qin, X. Yang, P. Zhang, Q. Wang, L. Zou, Y. Zhang, L. Zhang, Y. Fang, J. Li, H.-C. Zhou, *Adv. Mater.* **2018**, 30, 1704303; c)G. Zheng, S. de Marchi, V. Lopez-Puente, K. Sentosun, L. Polavarapu, I. Perez-Juste, E. H. Hill, S. Bals, L. M. Liz-Marzan, I. Pastoriza-Santos, J. Perez-Juste, *Small* **2016**, 12, 3935; d)K. Lu, T. Aung, N. Guo, R. Weichselbaum, W. Lin, *Adv. Mater.* **2018**, 30, 1707634.

[13] N. A. H. Md Nordin, A. F. Ismail, N. Yahya, *J. Teknol.* **2017**, 79.

[14] K. Shameli, M. B. Ahmad, A. Zamanian, P. Sangpour, P. Shabanzadeh, Y. Abdollahi, M. Zargar, *Int. J. Nanomedicine* **2012**, 7, 5603.

[15] a)D. M. Townsend, K. D. Tew, H. Tapiero, *Biomed. Pharmacother.* **2003**, 57, 145; b)S. Ma, Q. Huang, *RSC Adv.* **2015**, 5, 57847.

[16] K. Zhang, R. P. Lively, C. Zhang, R. R. Chance, W. J. Koros, D. S. Sholl, S. Nair, *J. Phys. Chem. Lett.* **2013**, 4, 3618.

[17] E. E. Sann, Y. Pan, Z. Gao, S. Zhan, F. Xia, *Sep. Purif. Technol.* **2018**, 206, 186.

[18] L. Litti, V. Amendola, G. Toffoli, M. Meneghetti, *Anal. Bioanal. Chem.* **2016**, 408, 2123.

[19] a)Y. MORIMOTO, Y. TERAO, K. ACHIWA, *Chem. Pharm. Bull.* **1987**, 35, 2266; b)Q. Zhou, B. Yan, W. Sun, Q. Chen, Q. Xiao, Y. Xiao, X. Wang, D. Shi, *Front. immunol.* **2021**, 12, 670427.

[20] S. Casey Laizure, V. Herring, Z. Hu, K. Witbrodt, R. B. Parker, *Pharmacotherapy* **2013**, 33, 210.

[21] J. I. Fletcher, M. Haber, M. J. Henderson, M. D. Norris, *Nat. Rev. Cancer.* **2010**, 10, 147.

[22] a)S. De Marchi, L. Vázquez-Iglesias, G. Bodelón, I. Pérez-Juste, L. Á. Fernández, J. Pérez-Juste, I. Pastoriza-Santos, *Chem. Mater.* **2020**, 32, 5739; b)C. Carrillo-Carrión, R. Martínez, M. F. Navarro Poupard, B. Pelaz, E. Polo, A. Arenas-Vivo, A. Olgiati, P. Taboada, M. G. Soliman, Ú. Catalán, S. Fernández-Castillejo, R. Solà, W. J. Parak, P. Horcajada, R. A. Alvarez-Puebla, P. del Pino, *Angew. Chem. Int. Ed.* **2019**, 58, 7078.